FERMILAB-Pub-88/189

Measurements of Radioactive Gaseous Releases to Air from Target Halls at a High Energy Proton Accelerator*

S. W. Butala, S. I. Baker and P. M. Yurista
Fermi National Accelerator Laboratory
P.O. Box 500, Batavia, IL 60510

December 1, 1988

*Submitted to Health Physics

Abstract

Measurements of induced radioactivity concentration in air were made at five target halls associated with the Fermilab high energy proton synchrotron. A gas flow-through ionization chamber was used to continuously sample air released from an exhaust stack at each location. The radioactive decay of a grab sample of air from each target hall was recorded and a best fit of each decay curve was made via iterative steps to determine the mixture of radionuclides present. The radionuclides ^{11}C, ^{13}N, ^{15}O, ^{38}Cl, ^{39}Cl and ^{41}Ar were identified. Two distinct radionuclide mixtures or "signatures" were found and were correlated to the geometry of the proton loss point. The normalized activity release rates for the five target areas agree within a factor of 2 of the average value of 2.7 $\mu Bq\ proton^{-1}$ for 800 GeV protons.

Introduction

The Fermi National Accelerator Laboratory (FNAL) superconducting proton accelerator, or Tevatron, has directed proton beams of up to 800 GeV to targets in 14 separate beamlines. Some of these beamlines have been in operation since the early 1970's when 200 GeV protons were first extracted from the Main Ring synchrotron. Historically, about half of the protons extracted from the accelerator have been directed to a single beamline used for neutrino experiments. The air ventilation exhaust stack at this beamline's target hall has been continuously monitored by a Geiger-Mueller (GM)-based gas sampling system as part of the environmental monitoring program. This system consists of a thin-window GM probe, mounted inside an airtight lead shielded container, through which air is pumped from the sample point (Butala and Baker 1988). Early measurements of the decay rate of air grab samples from the Neutrino target hall revealed an approximately 20 minute half-life; it has been concluded that ^{11}C was the dominant gaseous radionuclide released (Baker 1974). During 1978, the period of highest proton target intensity, the neutrino stack released 88.8 TBq (2.4 kCi) of ^{11}C. The corresponding dose equivalent at the FNAL site boundary has been calculated as 7 μSv (0.7 mrem) (Baker 1979).

Between 1984 and 1987, several new target halls began operation with 800 GeV protons. Also, the Anti-proton target hall, AP0, which produces antiprotons for the Tevatron Collider began operation with 120 GeV protons in 1985. This report describes measurements of air activity concentrations and attempts to characterize the gaseous radionuclide mixtures released from several target areas. No evaluation of radioactive aerosol releases was made. It is believed that radionuclides released in this form are less likely to remain airborne than gaseous effluents and thus have a much lower potential to contribute to the offsite collective dose equivalent.

Procedure and Measurements

Measurements of activity concentration were made with a Triton 955B* flow-through ion chamber. At each target hall, a plastic sampling tube of 6.35 mm inside diameter was inserted into the exhaust stack and run 12 m - 110 m to the location of the measuring apparatus. The Triton utilizes a 0.5 micron pore filter as well as an electrostatic filter to remove particulates and air ions so only air gases reach the ion chambers. Air was pulled through two 5 liter ion chambers which were connected in series before being exhausted outdoors. The flow rate was set to 4-6 L min^{-1}, so sampled air would reach the detector in less than 1 minute. Two identical sealed ion chambers continuously monitored the background radiation which was electronically subtracted from the current measured by the air sampling chambers.

The Triton had been calibrated against a known activity of tritiated methane several weeks before and after the field measurements. All measurements done in this study used this instrument's tritium (^{3}H) scale. Following the work of Peetermans, Triton response to accelerator produced air radionuclides is assumed to be a factor of five greater than that for ^{3}H (Peetermans 1972). This is based upon the higher average ß energy, typically > 0.5 MeV, of these radionuclides compared to the 5.68 keV average ß energy for ^{3}H. Thus, all measurements of activity concentration have been divided by 5 to convert from ^{3}H response.

At each sample location, air monitoring was done for a sufficiently long time period to assure that a steady-state activity concentration had been reached. This condition would typically be achieved after an hour of continuous beam operation. No additional buildup of longer lived radionuclides occurred since the target halls are ventilated to provide approximately 1-2 air exchanges per hour. Proton beam intensity to the targets was recorded via secondary emission

---

* Becton Dickinson Diagnostic Instrument Systems, 383 Hillen Rd., Towson, MD 21204

monitors (SEM's) which are normally located in the beam directly upstream of the target.

A representative grab sample of air was collected at each location by simply turning off the air pump, and then connecting the Triton inlet hose to the exhaust outlet. The radioactive air in this closed loop was allowed to decay within the ion chambers until no net counts above background were recorded. The Triton's counting electronics were input to a scaler which would integrate counts over a 56.3 second or 60 second time period. The former time increment corresponds to the Tevatron machine cycle. Scaler results were written to floppy disk and/or printed out, then entered into a personal computer spreadsheet program. The decay rate as a function of time was plotted and a best fit of each sample's decay curve was made via iterative steps, assuming that the radionuclides which might be present include ^{3}H, ^{11}C, ^{13}N, ^{15}O, ^{38}Cl, ^{39}Cl and ^{41}Ar. These have been identified in air at other particle accelerators. The radionuclides are produced by primary protons as well as secondary particles via spallation, (γ, n) and thermal capture reactions (Rindi and Charalambus 1967), (Höfert 1969), (Baarli and Peetermans 1974), (ICRU 1978), (Moritz 1987). Production of ^{38}Cl and ^{39}Cl via the (γ, pn) and (γ, p) reactions with ^{40}Ar has also been reported (Vialettes 1969). Activated air radionuclides with half-lives less than two minutes were not considered, since the time delay between activity production and subsequent detection by the Triton ranged from about 5 to 20 minutes. Table 1 lists these radionuclides along with their half-lives and principal decay modes.

Results and Discussion

Air activation measurements were made at five separate target halls. Four of the halls, N01, NM2, PB4 and MW6 targeted 800 GeV protons at intensities of 2-6 x 10^{12} protons pulse^{-1} on a 56.3 second cycle. The AP0 hall targeted 120 GeV protons at an intensity of 10^{12} protons s^{-1} on a 5 second cycle.

Figures 1-5 show the decay curve and best fit for each area's air grab sample. The error bars on the measured data represent the 95% confidence limit based on counting statistics only.

Table 2 summarizes the radionuclide mixture determined for each target hall and the total activity release rate as measured at each hall's exhaust stack. An alternate value of release rate is also reported for AP0 where it has been normalized to an 800 GeV proton energy to allow comparison with the other four target areas. Here, the value of activity release rate has been scaled linearly by a factor of 800 / 120 = 6.67.

The MW6 target area did not have an exhaust stack, so the measurement was done at the access gate to the target pile cave where air exhausted into a 4.5 x 10^4 m^3 building. This building, which houses four target piles, also lacks a release stack but exhausts its air outdoors via a multitude of leak points. Due to the proximity of the access penetration to the target pile, activity concentration measured at MW6 is estimated to have reached the sample point 5 minutes after being produced. This allowed the detection of a significant fraction of ^{15}O in the total gas mixture. The second set of MW6 data in Table 2 has been normalized to a 15 minute delay period, comparable to that of the other four target areas. The ^{15}O activity is virtually eliminated and the remaining proportion of ^{11}C and ^{13}N is similar to that measured at N01.

It is standard practice to continuously ventilate all FNAL beamline areas. This is mainly done to assure that good breathable air is present in the event that an access by personnel is required. Target station enclosures are designed to be at a net negative pressure to minimize leakage of potentially radioactive air into adjoining sevice buildings via access penetrations and cable ducts. Exhaust stacks are generally located at a point distant from the target station to provide a 10 - 20 minute delay period during which short-lived radionuclides may decay.

None of the air grab samples had measurable activity after several hours of decay, so it is concluded that no significant concentration of ^{3}H was generated. This is consistent with its very long half-life compared to the other radionuclides

measured in this study. This finding is also supported by vegetation sampling results near the AP0 and N01 exhaust stacks which indicate that the ^{3}H air release concentration is at least a factor of 10^{6} lower than that for ^{11}C (Baker 1988).

As seen in Table 2, the AP0 and NM2 halls revealed identical radionuclide mixtures, while the mixture found at PB4 is very similar. The mixtures determined for MW6 and N01 are similar to each other, but lack any of the longer lived radionuclides seen at the other three locations. An understanding of these results requires an examination of the five target systems.

As shown in Fig. 6, the target systems at AP0, NM2 and PB4 utilize thick steel shielding having > 800 g cm^{-2} radial and > 4000 g cm^{-2} longitudinal thickness around their target, magnets and proton dump. This geometry allows the hadronic showers to fully develop within the shields. Primary protons as well as secondary radiations activate air in the central cores of the shield piles, which contain the targets, transport magnets and dumps. These air volumes have cross sectional areas of about 1 m x 0.7 m and range in length from 7 m - 23 m.

The stations at AP0, NM2 and PB4 depart somewhat from what is depicted in Fig. 6. AP0 uses a shorter "lithium lens" as a focussing magnet, rather than the two dipoles shown. NM2 has a 10 meter air gap between its target pile and proton dump. The PB4 target pile uses three dipole magnets.

At AP0 and NM2, the target pile internal air volumes mix well with the air inside the target halls. The AP0 target system is ventilated by an exhaust fan which discharges air into the beamline enclosure. The NM2 target system has openings at the front and rear faces of its shield piles which allow ample mixing of air from within and outside the shields. The construction of the PB4 target station is much more airtight, which limits the mixing of air from within the PB4 shield with that inside the target hall building. This may be responsible for the observed difference in radionuclide ratio at PB4 versus that measured at AP0 and NM2. The relative concentrations of ^{11}C and ^{13}N at PB4 are lower than those measured at AP0 and NM2.

All three areas have air volumes external to their iron shields, which are activated by secondary radiations which escape the shields. These air masses mix with air from within the target piles before being released at the target hall exhaust stacks. In another study, measurements made *outside* a similarly massive iron shield revealed a neutron energy spectrum from thermal to a few hundred MeV, with a peak in the range of 1 keV - 1 MeV (Elwyn and Cossairt 1986). This "iron window" spectrum was concluded to be due to the small inelastic cross section of iron for neutrons with energies below 1 MeV. The significant presence of ^{41}Ar at the AP0, NM2 and PB4 target halls is indicative of a large thermal neutron component to the ambient radiation inside these target halls. The thermal neutron cross section for the reaction, $^{40}Ar(n,\gamma)\,^{41}Ar$, is 660 mb (Garber and Kinsey 1976). In addition to the thermal neutrons exiting the shield, it is likely that many intermediate energy (1 keV - 1 MeV) neutrons underwent elastic collisions with hydrogen nuclei in the target halls' concrete walls, ceilings and floors and were scattered back into the hall with thermal energies.

In contrast to the results found at AP0, NM2 and PB4, the longer lived radionuclides ^{41}Ar, ^{39}Cl and ^{38}Cl were completely absent at MW6 and N01. The MW6 target pile is very similar to those at AP0, NM2 and PB4, except that the exterior of its iron shielding is completely covered with concrete shield blocks (see Fig. 6). This outer layer of concrete is flush with the steel pile, which eliminates any appreciable air spaces. Thus, no significant air activation would be generated at the outer surface of the thick iron shield. This suggests that the production of ^{41}Ar, ^{39}Cl and ^{38}Cl at AP0, NM2 and PB4 occurred in the air volumes external to their thick iron shields.

The prompt radiation fluence rate emerging from the 660 g cm^{-2} heavy concrete shield surrounding the MW6 pile is many orders of magnitude lower than that inside the pile core and target hall. This shield was designed to allow unrestricted personnel access in its vicinity during beam operation. Not surprisingly, no air activation products were detected outside the pile other than a dilution of those which had leaked from the access penetration.

Radioactive air sampled at MW6 may have originated from two separate sources. The larger source is within the central core of the shield pile, where primary protons as well as secondary radiations traverse a 15 m air column following the one interaction length target. Secondary radiations also interact in the air volume surrounding the target and transport magnets. Convection air currents drain air from this channel into the concrete shield cave directly upstream of the target. The second, smaller source is a transport magnet known to have caused proton beam scraping losses, located approximately 25 m upstream of the pile. This iron and copper magnet had dimensions of 1.5 m long by 0.3 m radially thick. Secondary radiations, i.e. high energy hadrons, photons and evaporation neutrons may have activated the surrounding air.

Monte Carlo calculations predict that the shape of the neutron spectrum for a "thin iron" shield such as these transport magnets would be roughly 1/E with a peak in the range 1 keV - 1 MeV (Armstrong and Alsmiller 1969). A comparison of "thick iron" and "thin iron" shields indicates that the ratio of intermediate to high energy neutrons would be reduced by two orders of magnitude for the "thin" case (Alsmiller and Barish 1973), (Gollon 1976). Thus, the relatively thin iron yoke of a transport magnet would not be expected to degrade many neutrons to energies low enough to allow thermal capture by ^{40}Ar to produce ^{41}Ar. Apparently, the number of thermal albedo neutrons scattered off the concrete cave walls was insignificant compared to the high energy radiations which produced the measured radionuclides at MW6.

The other target hall which produced no measurable ^{41}Ar, ^{39}Cl or ^{38}Cl is N01. Here the neutrino Triplet train targeted 800 GeV protons on a one interaction length target, followed by an aluminum collimator having dimensions of 15 cm x 15 cm x 4 m (see Fig. 6). The target and collimator had iron shields of 120 g cm^{-2} and 320 g cm^{-2} maximum radial thickness, respectively. The proton beam traversed a 7 m long air path in this region. Beyond this point the uninteracted protons traveled 570 m in a vacuum pipe to an iron beam dump buried in the earth. Thus, the N01 hall did not have any beam loss points with

sufficient radial thickness to allow full development of the hadronic cascade.

While not completely clear from this study why production of ^{39}Cl and ^{38}Cl is only detectable for the target stations having "thick iron" geometries, it appears to be related to the expectation that the particle fluence rate outside a "thick iron" shield consists of a relatively large number of low energy particles while that for a "thin iron" geometry is characterized by a relatively small number of much higher energy particles. Production of ^{11}C and ^{13}N may be chiefly due to high energy spallation reactions on oxygen and nitrogen within the central cores of the target shields, while ^{39}Cl and ^{38}Cl are mainly produced outside "thick iron" shields by (n,pn) and (n,2np) reactions with atmospheric argon, respectively. It is possible that the photonuclear reactions, ^{40}Ar (γ ,p) ^{39}Cl and ^{40}Ar (γ ,pn) ^{38}Cl also occur. However, due to the relatively short radiation length for iron when compared to its nuclear interaction length, it is expected that neutrons would be the predominant radiation exiting the "thick iron" shields.

The absence of ^{41}Ar, ^{39}Cl and ^{38}Cl at MW6 might be explained as being due to the negligible volume of air and hence low number of available ^{40}Ar target atoms external to the iron shield pile. At MW6, concrete has been substituted for air. However, this condition is not the case at N01. An ample air volume surrounds the N01 target station to produce measurable quantities of ^{41}Ar, ^{39}Cl and ^{38}Cl. This air volume is only a factor of 4 smaller than those found at NM2 and PB4. Scaling these air volumes implies that at least 10% of the activity at N01 should have been due to ^{41}Ar, ^{39}Cl and ^{38}Cl. Since no such long lived radionuclides were detected, some other factor must be responsible. The only discernable difference is that N01 lacks a beam dump and its major proton loss point, i.e. target and collimator, have a relatively "thin" iron radial shield.

The contention that significant production of ^{41}Ar, ^{39}Cl and ^{38}Cl only occurs outside a radially "thick" iron shield is further supported by the results found at the PB4 target hall. During the construction of this target station, unusually great care was taken to eliminate gaps between its iron plates. Plates

were cut to closer tolerances, lead sheet was used to fill gaps and staggered plate stacking was done to assure no continuous voids existed. The major route of air exchange from within the pile to the target hall is a 10 cm diameter hole at the pile's front face, through which the proton beam is directed. This limits the air exchange rate compared to the conditions at NM2 and AP0. The gas mixture measured at the PB4 exhaust stack has a lower proportion of ^{11}C and ^{13}N than does NM2 or AP0. The ratio of ($^{11}C + ^{13}N$) / ($^{38}Cl + ^{39}Cl + ^{41}Ar$) is 0.67 at PB4, and 1.27 at AP0 and NM2. Since all other factors at PB4 are virtually identical to those at AP0 and NM2, it is concluded that the radioactive air generated external to the "thick iron" pile has significantly greater concentrations of ^{38}Cl, ^{39}Cl and ^{41}Ar.

Conclusion

Measurements of radioactive gas activity concentration released from five target halls revealed two distinct "signatures" of radionuclide mixture. The one associated with proton losses on radially "thin iron" shields (< 350 g cm^{-2}) was a mixture of ^{11}C and ^{13}N in about a ratio of $^{11}C / ^{13}N = 2.7$, with trace amounts of ^{15}O, as measured about 15 minutes after activation. This signature can be expected for losses on transport magnets and beam collimators. The signature for radially "thick iron" shields (> 800 g cm^{-2}) includes ^{11}C , ^{13}N, ^{38}Cl, ^{39}Cl and ^{41}Ar where the ratio of $^{11}C / ^{13}N = 3.0$ when measured about 15 minutes after production. At the same time reference, the ratio of activity concentration, ($^{11}C + ^{13}N$) / ($^{38}Cl + ^{39}Cl + ^{41}Ar$), is roughly unity. This signature would be expected for hadron losses on typical beam dumps, which lack appreciable hydrogen content.

When normalized per unit 800 GeV proton on target and to a time 15 minutes after activation, i.e. about the average time it takes for the activated air to reach the exhaust stack, the average stack release rate for the five locations is 2.7 μBq $proton^{-1}$ (73 aCi $proton^{-1}$). All measurements made in this study fall

within a factor of two of this value. A check of the linearity of the activity concentration released as a function of target intensity was made at N01. The results shown in Figure 7 indicate a very linear response over the factor of 4 beam intensity range.

In order to evaluate the relative effect on the peak annual offsite dose equivalent and the collective dose commitment to the public, two source terms were modeled using AIRDOS-EPA (Moore et al. 1979). The first was the "thin iron" gas mixture, comprised of 70% ^{11}C and 30% ^{13}N. The second was the "thick iron" mixture, modeled as 42% ^{11}C, 14% ^{13}N, 10% ^{39}Cl and 34% ^{41}Ar. The actual AP0 target area conditions during 1987 were modeled, which includes a stack release of 2.0 TBq (54 Ci). The same total activity was input for both gas mixtures considered. Also included were the meteorological conditions at the Fermilab site in 1986 and the surrounding population distribution for 1987. Obviously, these latter two conditions are highly specific so the final results can not be directly extrapolated to any other facility.

The results of this comparison are shown in Table 3. The computer code did not include ^{39}Cl in its library, so the contribution from this radionuclide was not evaluated. However, it represents the smallest fraction of total activity in the mixture and has a shorter half-life than does ^{41}Ar. The absence of ^{39}Cl from this model should have negligible effect on the results. It can be seen that the maximum dose equivalent at the site boundary is virtually the same for both cases, about 0.2 μSv (20 μrem). The peak dose equivalent at the site boundary occurred where the distance from the stack to the fencepost was at its minimum, about 1100 m.

The collective dose equivalent to the surrounding population within a 128 km (80 mi) radius of FNAL is about a factor of four greater for the case of the "thick iron" radionuclide mixture. As Figure 8 illustrates, the dose equivalent rate for the two different air radionuclide mixtures is nearly the same at radial distances < 10 km. Beyond 10 km, the ^{11}C and ^{13}N components have been greatly reduced and the dose is predominately due to ^{41}Ar.

Acknowledgments - The authors would like to thank Mr. Steven Benesch for development and construction of the remote data logger system which made it feasible to conduct the many grab sample decay measurements. We also wish to thank Mr. William Salsbury for performing the calculations of dose equivalent rate and annual collective dose equivalent using AIRDOS-EPA, and Drs. J. D. Cossairt and A. J. Elwyn for reviewing the manuscript and offering helpful suggestions.

References

Armstrong and Alsmiller 1969 Armstrong, T.W.; Alsmiller, Jr., R.G.; Oak Ridge National Laboratory Report: ORNL-TM-2498, 1069.

Alsmiller and Barish 1973 Alsmiller, Jr., R.G.; Barish, J.; Shielding against the neutrons produced when 400 MeV electrons are incident on a thick copper target. Particle Accel. Vol. 5, p.155, 1973.

Baarli and Peetermans 1974 Baarli, J.; Peetermans, A.; Air radioactivity from the CERN accelerator installations. CERN Health Physics Group, Report DI/HP/176, 1211 Geneva 123, Switzerland; February 15, 1974.

Baker 1974 Baker, S. I.; Environmental monitoring report for calendar year 1973. Fermilab Report, March 15, 1974. Fermilab, P.O. Box 500, Batavia, IL 60510.

Baker 1979 Baker, S. I.; Environmental monitoring report for calendar year 1978. Fermilab Report - 79/26, 1104.100, May 1, 1979. Fermilab, P.O. Box 500, Batavia, IL 60510.

Baker 1988 Baker, S. I.; Environmental monitoring report for calendar year 1987. Fermilab Report - 88/40, 1104.100, UC-41, May 1, 1988. Fermilab, P.O. Box 500, Batavia, IL 60510.

Butala and Baker 1988 Butala, S. W.; Baker, S. I.; Calibration of the N01 stack monitor. Radiation Physics Note 68, FNAL Safety Section, March 1988. Fermilab, P.O. Box 500, Batavia, IL 60510.

Elwyn and Cossairt 1986 Elwyn, A. J. and Cossairt, J. D.; A study of neutron leakage through an Fe shield at an accelerator. Health Phys., Vol. 51, No. 6, pp. 723-735, December 1986.

Garber and Kinsey 1976 Garber, D.I. and Kinsey, R.R.; Neutron cross sections, vol. II, curves, National Neutron Cross Section Center, Brookhaven National Laboratory, Upton, NY 11973, Report: BNL 325

Gollon 1976 Gollon, P. J.; Dosimetry and shielding factors relevant to the design of iron beam dumps. FNAL TM-664, March 17, 1976, Fermilab, P.O. Box 500, Batavia, IL 60510.

Höfert 1969 Höfert, M.; Radiation hazard of induced activity in air as produced by high energy accelerators. Proceedings of the second international conference on accelerator dosimetry and experience; November 5-7, 1969, Stanford, CA; CONF-691101, pp. 111-119.

ICRP 1983 International Commission on Radiological Protection. Radionuclide transformations. Oxford: Pergamon Press; ICRP Publication 38, Ann. ICRP, Vols. 11-13, 1983.

ICRU 1978 International Commission on Radiation Units and Measurements. Basic aspects of high energy particle interactions and radiation dosimetry. 7910 Woodmont Ave., Washington, D.C. 20014: ICRU Report 28; 1978 p. 38.

Moore et al. 1979 Moore, R.E.; Baes III, C. F.; McDowell-Boyer, L.M.; Watson, A. P.; Hoffman, F. O.; Pleasant, J. C. and Miller, C. W.; AIRDOS-EPA: A computerized methodology for estimating environmental concentrations and dose to man from airborne releases of radionuclides. Oak Ridge National Laboratory Report ORNL-5532, June 1979.

Moritz 1987 Moritz, L.E.; Air activity and its control at a 500 MeV meson production facility. Proceedings of the twentieth midyear topical symposium of the Health Physics Society; 8-12 February 1987; Reno, NV: CONF-8602106, available from NTIS, U.S. Dept. of Commerce, Springfield, VA 2216.

Peetermans 1972 Peetermans, A.; Calibration experimentale et calculee des chambres d'ionisation a circulation d'air. CERN Report 72 - 12, CERN, 1211 Geneva 23, Switzerland, July 4, 1972.

Rindi and Charalambus 1967 Rindi, A. and Charalambus, S.; Airborne radioactivity produced at high-energy accelerators. Nucl. Instr. Meth. 47, 1967, p. 227.

Vialettes 1969 Vialettes, H.; Gas and dust activation in the target room of the Saclay electron linac. Proceedings of the second international conference on accelerator dosimetry and experience; November 5-7, 1969; Stanford, CA; CONF-691101, pp. 121-136.

Table 1. Gaseous radionuclides with half-lives > 2 minutes which have been identified in air at various high energy particle accelerators.

Radionuclide	Half-life	Principal Decay Modes	Energy (MeV)	Mode Frequency (transformation^{-1})
^{3}H	12.35 y	β^-	5.68 x 10^{-3}	1.0
^{11}C	20.38 min	β^+	0.385	0.998
		γ	0.511	2.0
^{13}N	9.97 min	β^+	0.492	0.998
		γ	0.511	2.0
^{15}O	2.04 min	β^+	0.735	0.999
		γ	0.511	2.0
^{38}Cl	37.21 min	β^-	0.420	0.325
		β^-	1.181	0.114
		β^-	2.244	0.561
		γ	1.642	0.325
		γ	2.168	0.440
^{39}Cl	55.6 min	β^-	0.346	0.023
		β^-	0.408	0.026
		β^-	0.789	0.831
		β^-	0.907	0.043
		β^-	1.528	0.070
		γ	0.250	0.470
		γ	0.986	0.022
		γ	1.091	0.026
		γ	1.267	0.540
		γ	1.517	0.380
^{41}Ar	1.83 h	β^-	0.459	0.992
		γ	1.294	0.992

All β energies listed are average values. Physical data is as published in ICRP Publication 38 (ICRP 1983).Transitions which occur with a frequency less than 1% have been omitted.

Table 2. Gaseous air activation products and release rates measured at proton target hall exhaust stacks.

Target hall	Relative ratio of measured activity concentration						Normalized release rate of total activity (μBq proton^{-1})
	^{11}C	^{13}N	^{15}O	^{38}Cl	^{39}Cl	^{41}Ar	
AP0	42	14	0	0 [a]	10	34	0.5 (3.3) [b]
MW6 [c]	46	19	35	0	0	0	10.5
MW6 [d]	75.5	22	2.5	0	0	0	4.5
N01	65	32	3	0	0	0	1.9
NM2	42	14	0	0	10	34	2.5
PB4	30	10	0	10	30	30	1.3

a The decay rate fit did not reveal the presence of ^{38}Cl. A subsequent gamma spectroscopy measurement made with a portable intrinsic Ge detector in the airstream of the exhaust stack indicated that ^{38}Cl was present. The relative ratio of activities measured for ^{38}Cl : ^{39}Cl : ^{41}Ar is 25:31:44.

b This value has been scaled linearly from actual value measured during 120 GeV operation, to normalize for an 800 GeV proton energy.

c Values reported in this row are those actually measured at a time estimated to be 5 minutes following activation.

d Values reported in this row have been extrapolated from measured values, above, allowing an additional 10 minutes of radioactive decay.

Table 3. Maximum annual dose equivalent at site boundary and collective dose equivalent to surrounding population as calculated for two radionuclide mixtures having approximately equal activity release rates.

Modeled gas mixture released from AP0 stack	Maximum annual dose equivalent at Fermilab site boundary	Collective dose equivalent to population within 128 km radius of Fermilab
"Thin iron" mixture: 1.4 TBq ^{11}C 0.6 TBq ^{13}N	0.20 μSv (20 μrem)	0.83 person-mSv (0.083 person-rem)
"Thick iron" mixture: 0.84 TBq ^{11}C 0.28 TBq ^{13}N 0.68 TBq ^{41}Ar	0.21 μSv (21 μrem)	3.5 person-mSv (0.35 person-rem)

List of Figure Captions

Fig. 1. Radioactive decay measurement of air grab sample from release stack at AP0 target hall.

Fig. 2. Radioactive decay measurement of air grab sample from access labyrinth at MW6 target hall.

Fig. 3. Radioactive decay measurement of air grab sample from release stack at N01 target hall.

Fig. 4. Radioactive decay measurement of air grab sample from release stack at NM2 target hall.

Fig. 5. Radioactive decay measurement of air grab sample from release stack at PB4 target hall.

Fig. 6. Elevation views of target stations. Stations at AP0, NM2 and PB4 resemble figure labeled 'A'. 'B' depicts MW6 target pile and 'C' shows N01 target area.

Fig. 7. Activity concentration released from N01 stack vs. 800 GeV proton flux on a 1 interaction length target.

Fig. 8. Dose equivalent rate as a function of distance from AP0 release stack for two different gas mixtures having approximately the same initial total activity. Mixture A represents release expected for a "thin iron" loss point. Mixture B is actual release from AP0 "thick iron" target station during 1987.

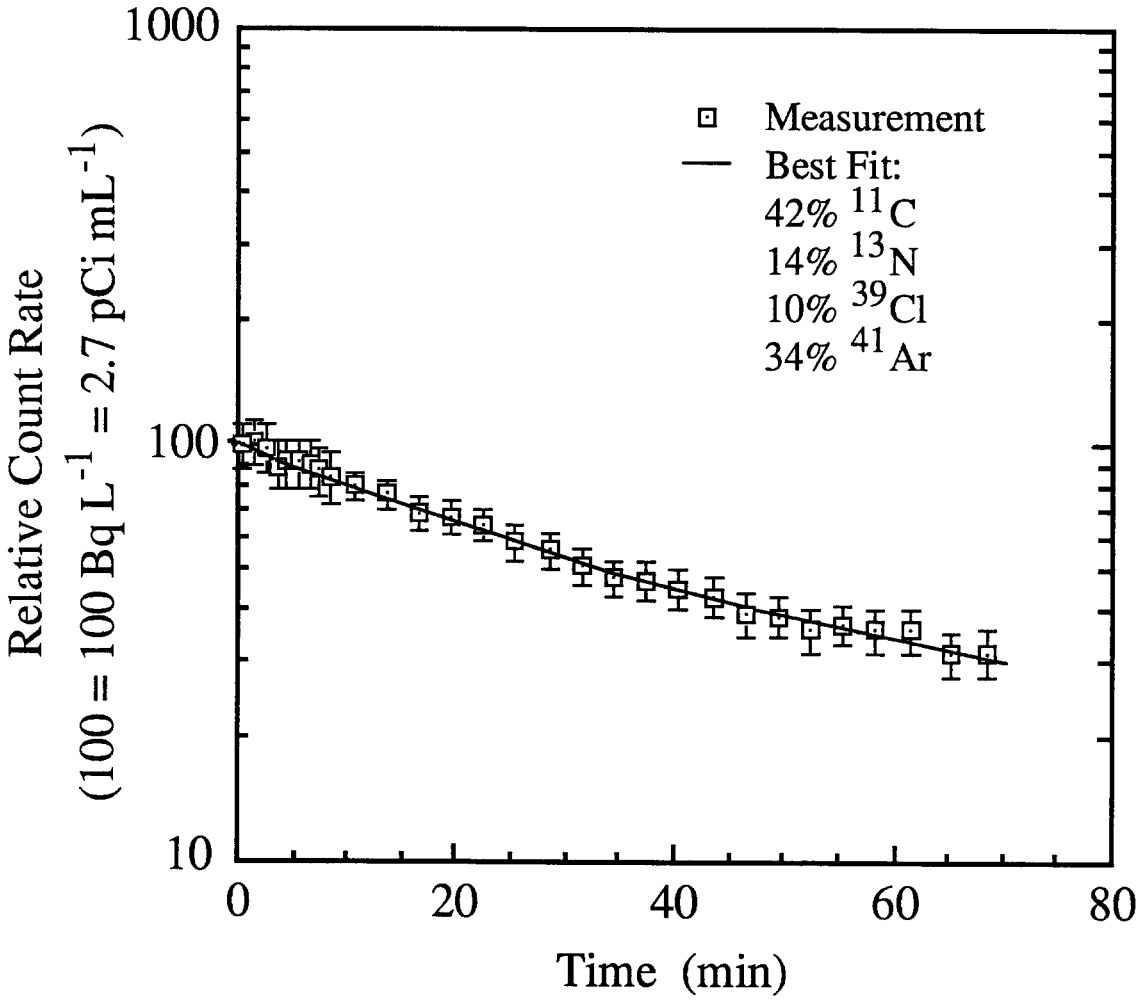

Fig. 1. Radioactive decay measurement of air grab sample from release stack at AP0 target hall.

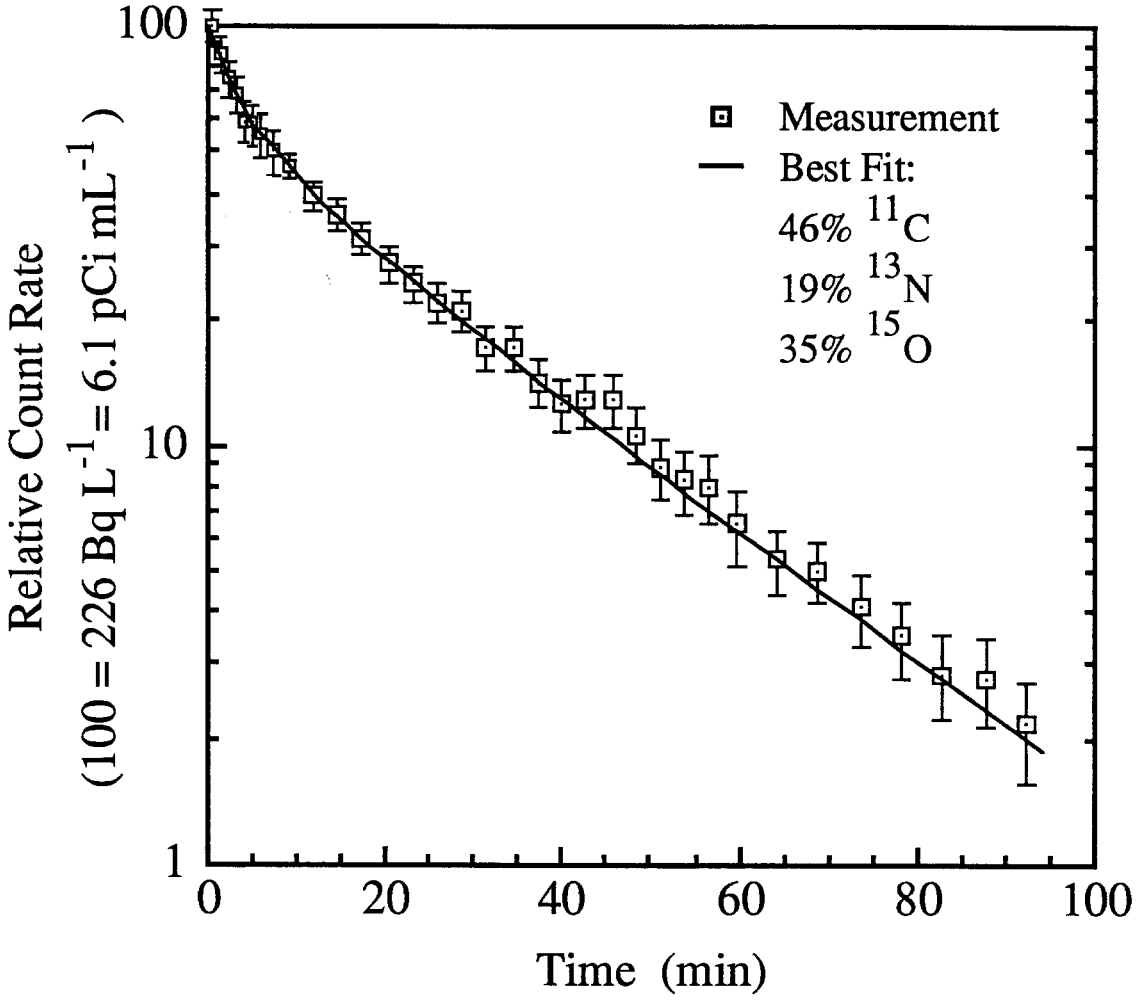

Fig. 2. Radioactive decay measurement of air grab sample from access labyrinth at MW6 target hall.

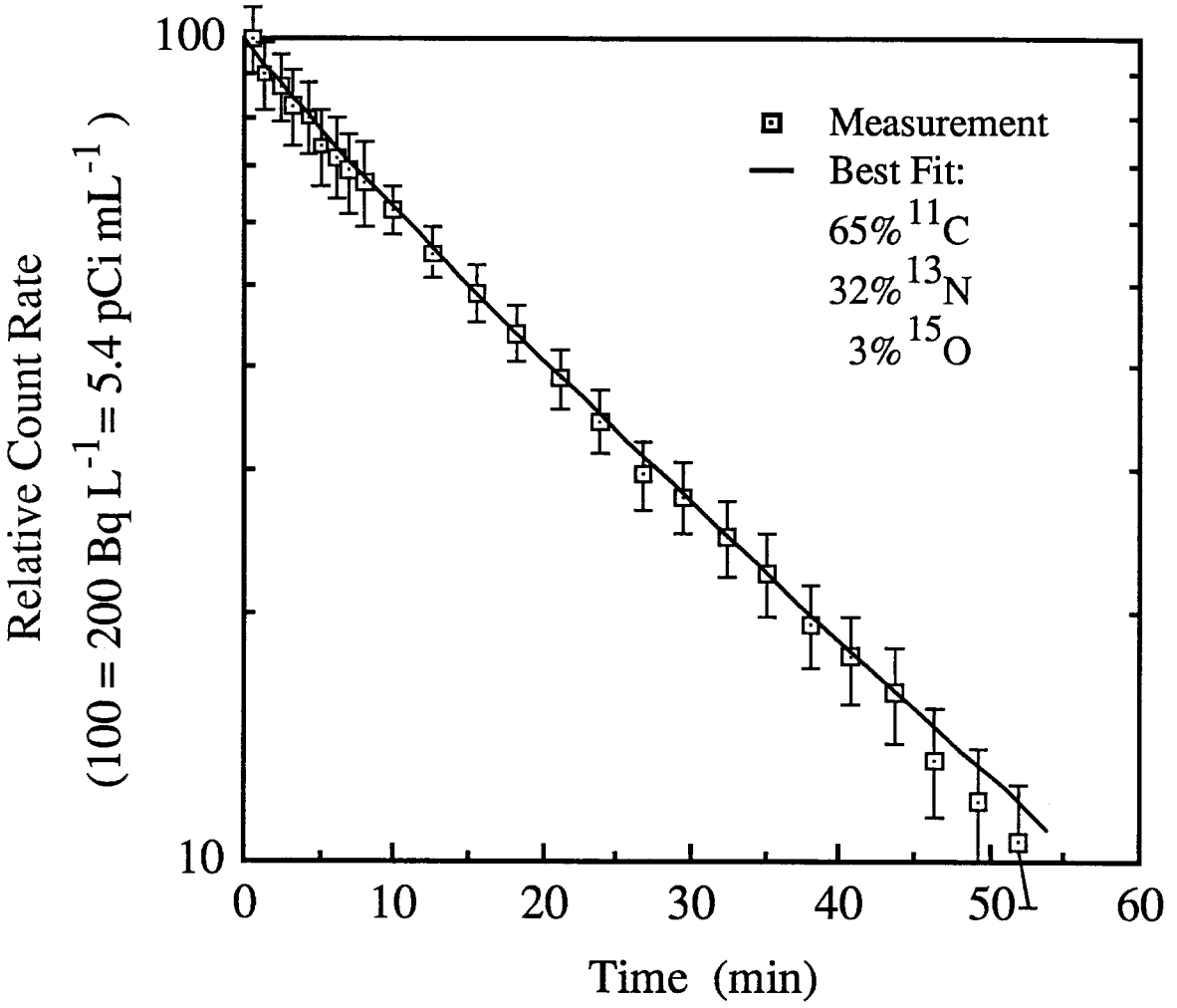

Fig. 3. Radioactive decay measurement of air grab sample from release stack at N01 target hall.

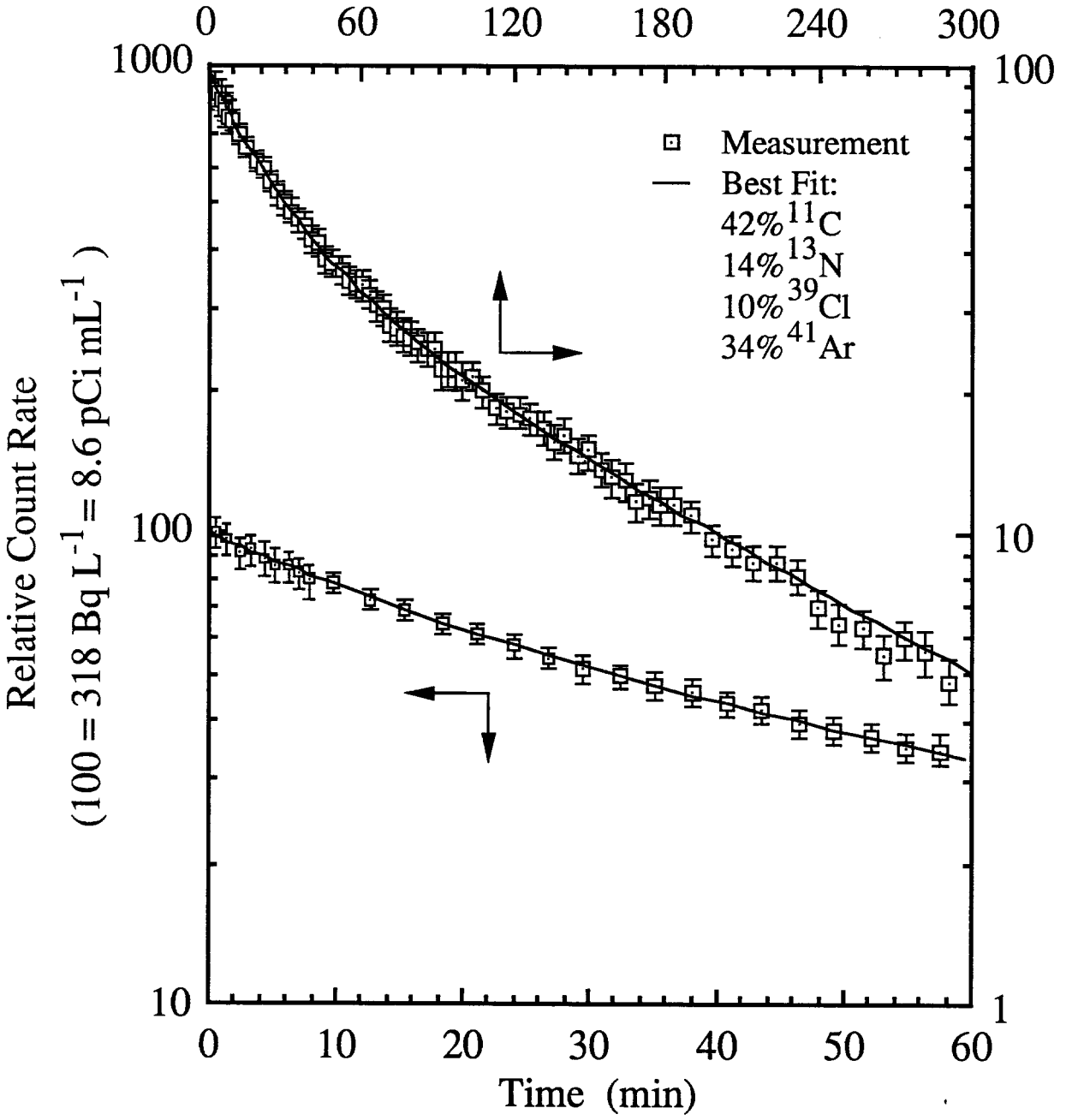

Fig. 4. Radioactive decay measurement of air grab sample from release stack at NM2 target hall.

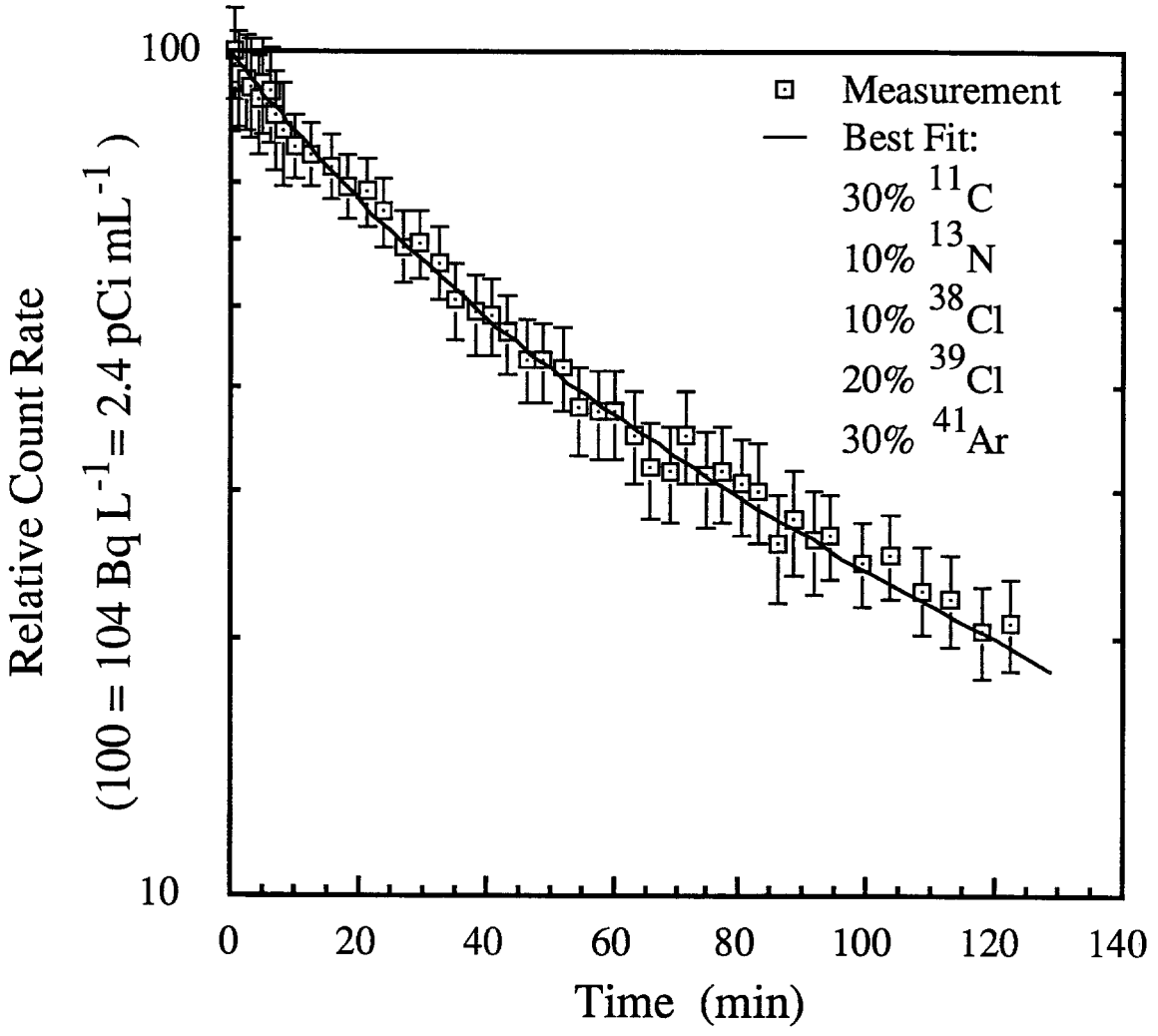

Fig. 5. Radioactive decay measurement of air grab sample from release stack at PB4 target hall.

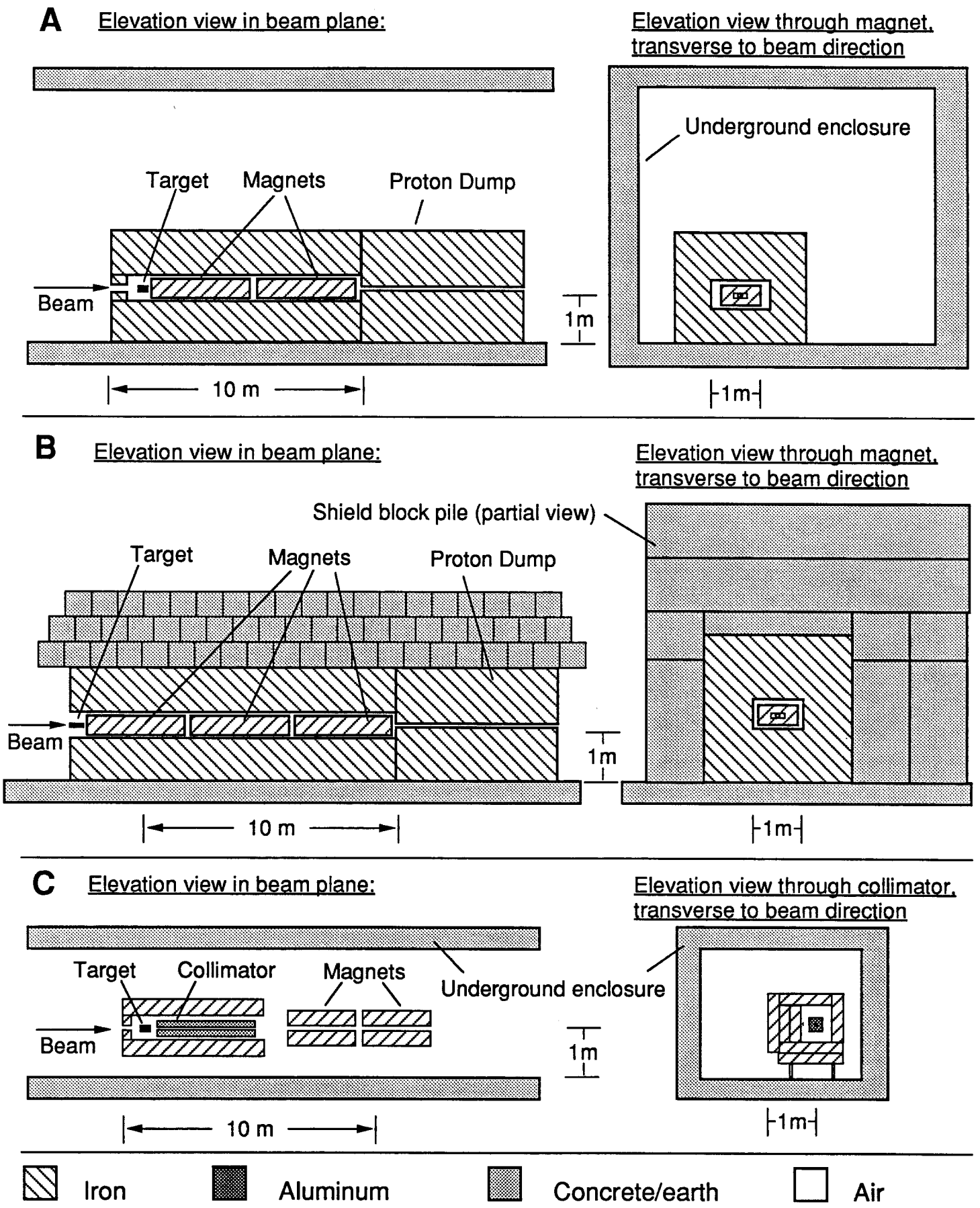

Fig. 6 Elevation views of target stations. Stations at AP0, NM2 and PB4 resemble figure labeled 'A'. 'B' Depicts MW6 and 'C' shows N01.

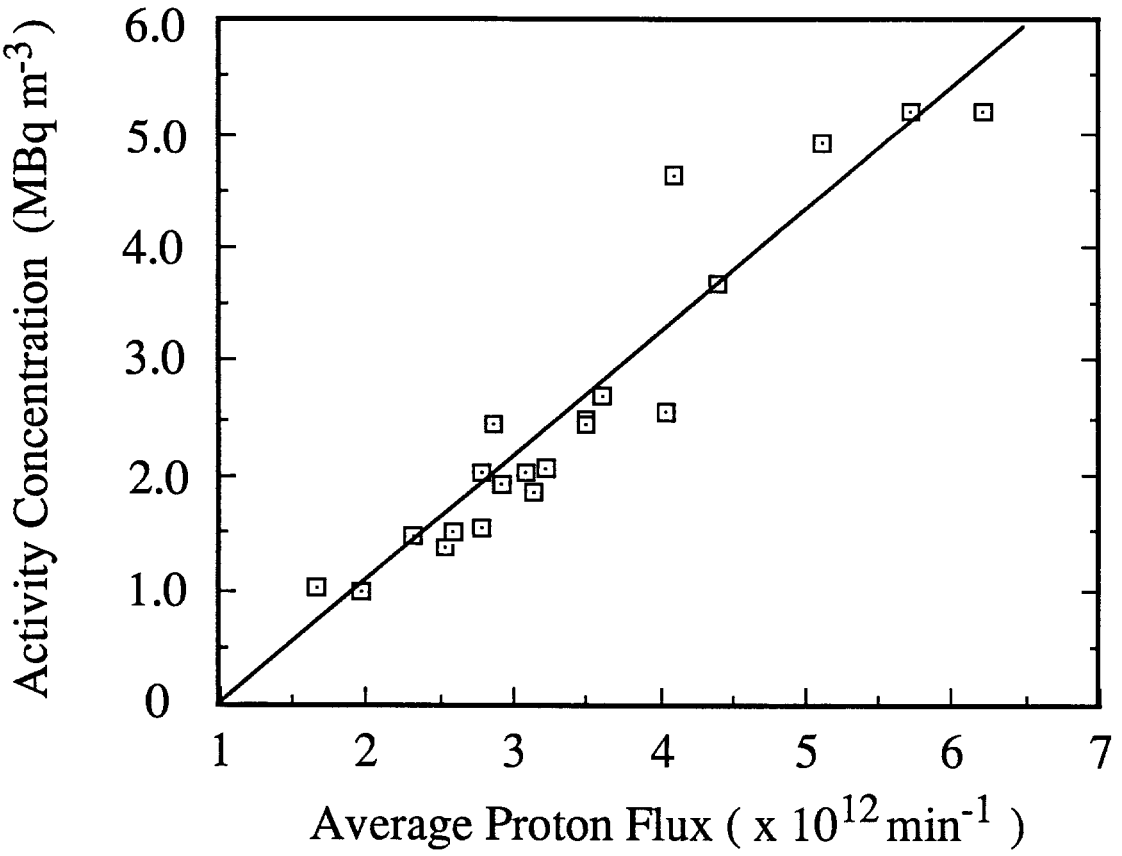

Fig. 7. Activity concentration released from N01 stack vs. 800 GeV proton flux on a 1 interaction length target.

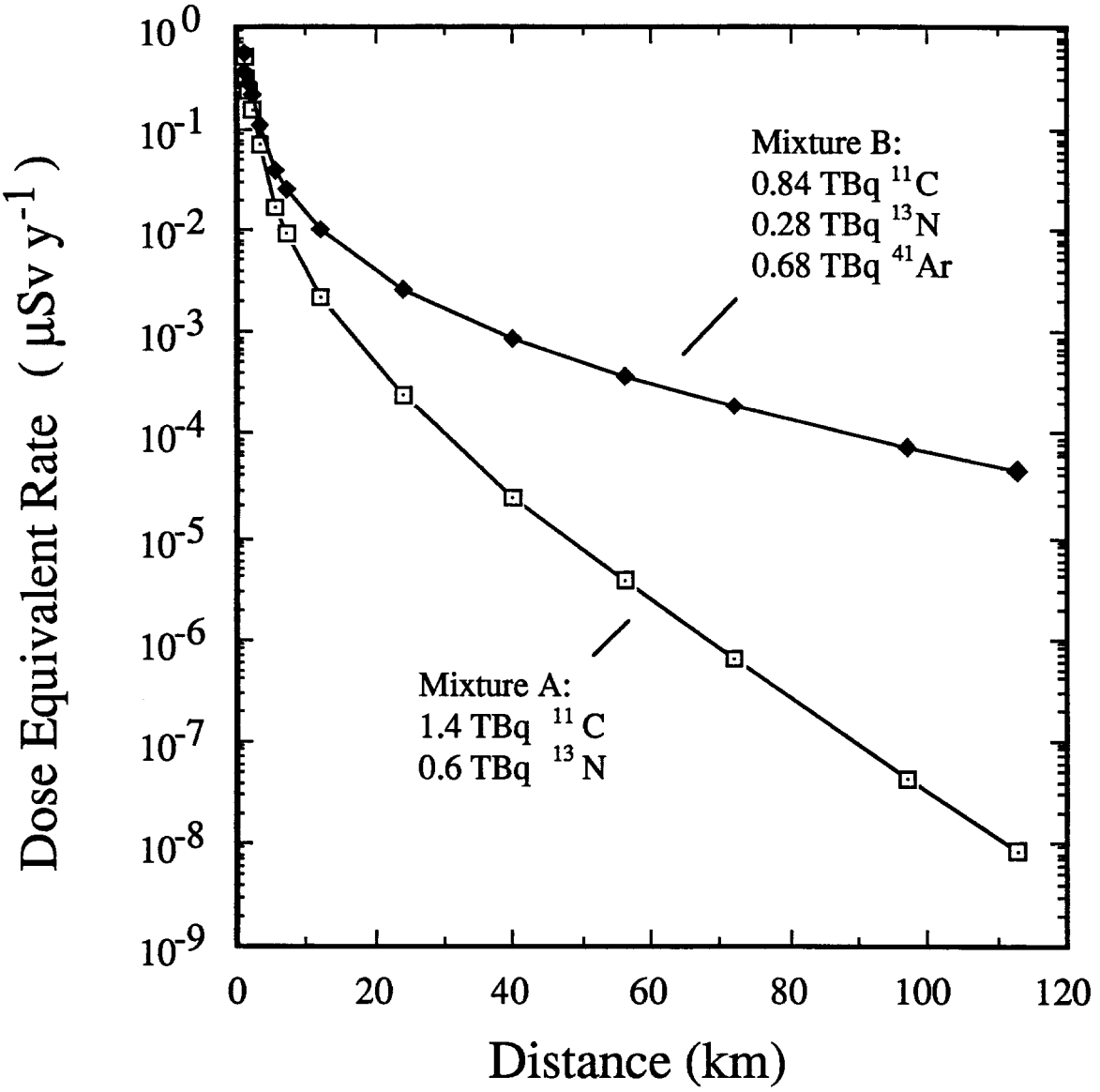

Fig. 8. Dose equivalent rate as a function of distance from AP0 release stack for two different gas mixtures having approximately the same initial total activity. Mixture A represents release expected for a "thin iron" loss point. Mixture B is actual release from AP0 "thick iron" target station during 1987.